

Influence of Small Amount of Cu Addition on Microstructure, Deformation Temperature, and the Tensile Behaviour of Sn-9Zn-1.5Ag Lead free Solder Alloy

M.Y. Salem

Physics Department, Faculty of Science, New Valley University, New Valley, 72511, El-Kharga, Egypt.

Sn-9Zn-1.5Ag and Sn-9Zn-1.5Ag-0.7Cu alloys have been inspected under different five strain rates ranging from $5.4 \times 10^{-5} \text{ S}^{-1}$ to $2.9 \times 10^{-3} \text{ S}^{-1}$ and different three temperatures extended from R.T. (298K) to 393 K for two alloys. The difference in thermal action, microstructure and stress-strain advantage related with addition of 0.7 Cu wt% was investigated. Transmission electronic microscope (TEM) investigation of samples revealed a homogenous uniform distribution, size refinement of IMCs and β -Sn grains. Addition of 0.7Cu particles into the Sn-9Zn-1.5Ag enhanced the yield stress σ_{YS} by 17% and reducing the ultimate tensile strength UTS by 12%. The addition of adding Cu was found to be lowering ductility (total elongation) by 19% of the Sn-9Zn-1.5Ag solder due to the refinement of β -Sn grains; this means that Sn-9Zn-1.5Ag-0.7Cu is more strengthening than Sn-9Zn-1.5Ag. The activation energy of Sn-9Zn-1.5Ag is lower than that of Sn-9Zn-1.5Ag-0.7Cu; therefore first sample is more superplastic.

1. Introduction

Sn based alloys are convenient for refinement electronics content connections as a lead-free composite welding [1]. Lately high-temperature solders have been great utilized in different pattern of usages like aggregation optoelectronic components, auto- mobile circuit boards, circuit modules for step soldering, etc. [2,3]. Sn-9Zn is the best solder alloy for most applications in optoelectronic packaging, because of its high creep resistance, wettability and good reliability [4,5]. Certainly, high soldering temperatures could damage the properties of optical fibers and sensitive optoelectronics such as lasers,

light emitting devices, photodetectors, or waveguide devices [6]. Significant tests have been done to improve a new propagation of solders with low melting point, Logical cost, elevated magnitude stability and supporting solder joints achievement with growing reduction and more input/output terminals [7].

Our tested alloys solder is one of great potential substitutional materials; it has a stable microstructure, good mechanical properties, high creep and corrosion strength and perfect solderability [8,9]. Solidification appear an essential effect because of it constitute the fundamental for improve the microstructure and consequently advance the samples quality; thus the output specimen and stabilization process possess a significant effectiveness on the feature and progressed the characteristics of cast metals [10,11]. The mechanical characteristic of the samples can be modified by gaining finer microstructure result from higher solidification rates and higher cooling rates under many solidification situations [12,13]. Liu et al. mentioned [14] that the stress-strain of the examined alloy is importantly elevated than that from the pre-tested alloy.

2. Experimental Procedures

Two alloys of compositions Sn-9Zn-1.5Ag and Sn-9Zn-1.5Ag-0.7Cu were prepared from Sn, Zn, Ag and Cu raw materials with purity 99.99 %. These raw elements are mixed in wt. % in ceramic crucible and melted at 450 °C for two hours. The dissolved material in the furnace is given in a mold of copper to be wire with the desired diameter. More details of composite alloys preparation are described elsewhere [15,16]. A cooling rate of 5-8⁰C/s was achieved, so as to create the fine microstructure typically found in small solder joints in microelectronic packages. To gain samples including the completely precipitated phases, the samples were annealed at 150 °C for 1 h, then left to cool quietly to room. This process is declaration to licence a little amount of grain growth and grain stabilization to occur [17,18]. The samples were examined at three temperatures ranging from 298K to 393 K for the two alloys a waiting time 10 min for the test temperatures to be reached, under different strain rate ranging from 5.4x10⁻⁵ S⁻¹ to 2.9x10⁻³ S⁻¹, using a computerized form creep machine [18]. The chemical structure of the examined samples is registered in Table (1). The accuracy of temperature measurement is of the order ± 1 K. Strain measurements were done with an accuracy of ±1x10⁻⁴. A solution of 2% HCl, 3% HNO₃ and 95% (vol.%) ethyl alcohol was prepared and used to etch the samples.

Table1: Chemical composition of the studied solder alloys (wt. %).

Solder alloy	Sn	Zn	Ag	Cu
Sn-9 Zn-1.5Ag	89.5	9	1.5	0
Sn-9Zn-1.5 Ag-0.7Cu	88.8	9	1.5	0.7

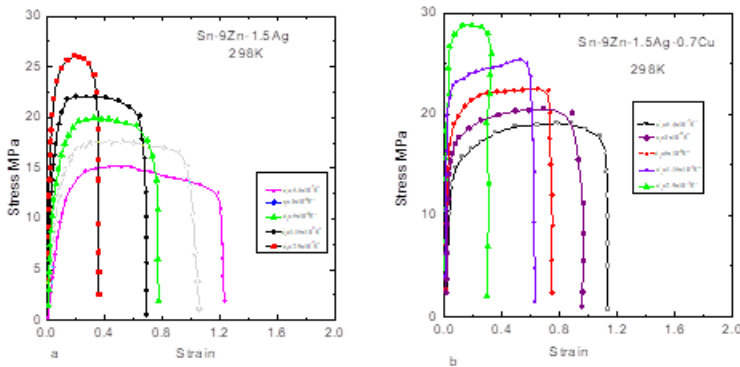


Fig.(1): Comparative tensile stress-strain curves obtained at 298K and different strain rate Sn-9Zn-1.5Ag and Sn-9Zn-1.5Ag-0.7Cu solder alloys

3. Results and Discussion

3.1. Mechanical Properties.

3.1.1. Tensile Properties

The relation of tensile curves for two tested alloys were illustrated in Figs.(1-3) at 298K, 333K, and 393 K at different five strain rates ranging from $5.4 \times 10^{-5} \text{ S}^{-1}$ to $2.9 \times 10^{-3} \text{ S}^{-1}$; it is obvious that at 298 K for the first sample Sn-9Zn-1.5Ag; the stress is about 26 MPa but for second alloy Sn-9Zn-1.5Ag-0.7 is about 28.8 MPa; while strain is 1.23 for the first one and 1.15 for the second one; this means that 0.7 increase strengthening for Sn-9Zn-1.5Ag.

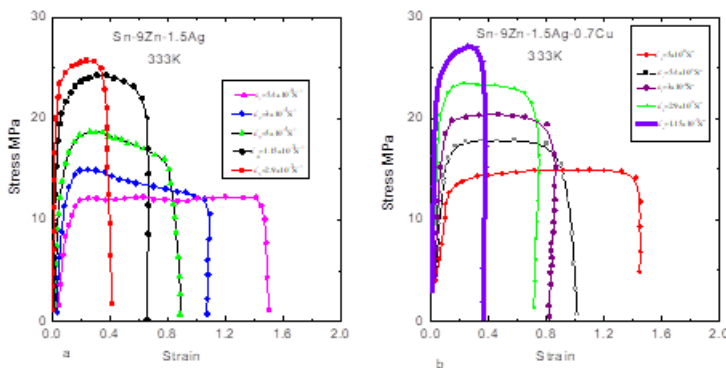


Fig.(2): Comparative tensile stress-strain curves obtained at 333K and different strain rate Sn-9Zn-1.5Ag and Sn-9Zn-1.5Ag-0.7Cu solder alloys

It is clear that strain hardening appear instead of strain

softening for all specimens due to 0.7 Cu addition, which can be owing to the strengthening mechanism of inter metallic compound stages in the alloy matrix. However, during strain hardening is preventing dislocation activity. As the dislocation intensity rises; the impedance to their movement propagates. It is shown that the stress enhances strain hardening [19].

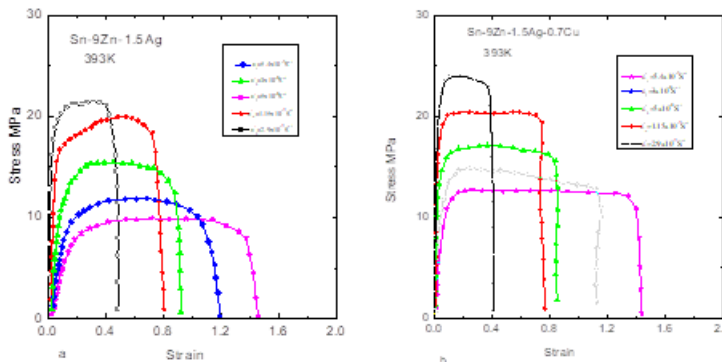


Fig.(3): Comparative tensile stress-strain curves obtained at 393K and different strain rate Sn-9Zn-1.5Ag and Sn-9Zn-1.5Ag-0.7Cu solder alloys

3.1.2. Influence of temperature and Young's modulus (y), yield stress (σ_y), and σ_f

Figure (4a, b) lists the variation of Young's modulus (Y) with strain rate at different working temperature for Sn-9Zn-1.5Ag and Sn-9Zn-1.5Ag -0.7 Cu. It is clear that Young's modulus (Y) for Sn-9Zn-1.5Ag samples is higher than that of Sn-9Zn-1.5Ag -0.7Cu samples by about 91%. It is evident that Young's modulus (Y) is rise with rising strain rate and temperature.

In Fig.5 the differentiation of the ultimate tensile stress (UTS) with strain rate the examined samples is represented; it is shown that (UTS) for is about 26 for Sn-9Zn-1.5Ag; but equal about 29 for second alloy see Fig.(5). The Variation of yield stress (σ_y) with strain rate at different working temperature for Sn-3.5Ag-0.7Cu, and Sn-3.5Ag-0.7Cu-0.3GO is shown in Fig.6; it is clear the yield stress (σ_y) for Sn-9Zn-1.5Ag solders is about 24.8 but for Sn-9Zn-1.5Ag-0.7Cu is about 29; this means that Sn-9Zn-1.5Ag-0.7Cu is more strengthening than Sn-9Zn-1.5Ag. It is evident that (UTS) and yield stress (σ_y) grow with growing strain rate and decrease with increasing temperature. Similar behaviour was observed by other researchers working on SAC and SC solders [20,21]. It was realized that at summit corresponding temperatures, the elongation of the material does not permanently decrease or increase with either a decrease or increase in the T and ϵ : [22].

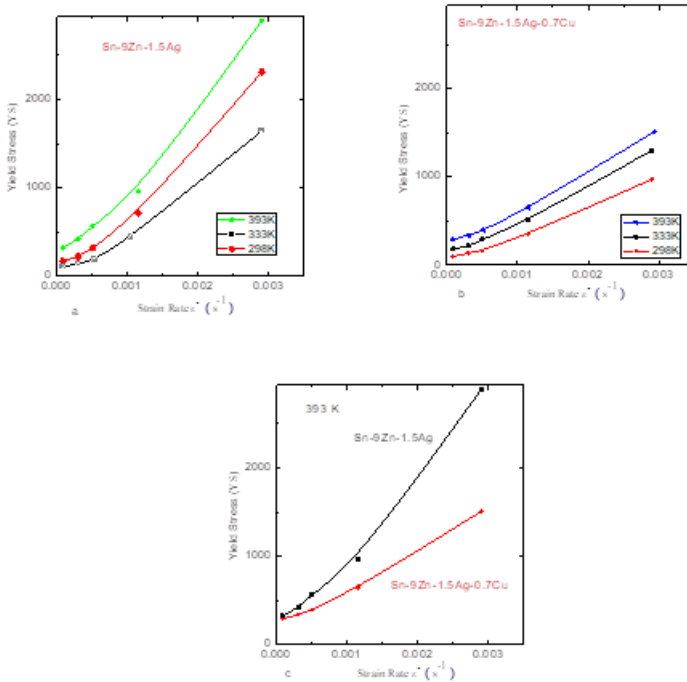


Fig.(4) a, b : The comparison of Young's modulus (Y) with strain rate at different working temperature for tested solder alloys; c) The comparison of (Y) at fixed temperature 393 K.

To understand that you should consider must study IMC; additional development was developed by Ashby and Edward [23] to study creep damage and failure of different materials that are degraded due to the failure of high temperatures results from different mechanisms [23].we must know that the mechanisms of damage are varied, and there are several explanations for the sensitivity of ductility in temperature testing, affect the structural effects, treatment and separation of impurities [24,25].

The relationship through the fracture strength (breaking strength) σ_f and strain rate at various working temperature has been examined in Fig.(7a,b); but in It is obvious that fracture strength (σ_f) for Sn-9Zn-1.5Ag-0.7 Cu is more than that of Sn-9Zn-1.5Ag; this means that Sn-9Zn-1.5Ag is extreme elongation. The strain rate reliance of the total elongation ϵ_t was constructing to follow an experimental equation of the form [26]:

$$\epsilon_t = A \exp(-\lambda \epsilon) \tag{1}$$

where A and λ are fixed constant depending on the tensile test situation.

The total strain of two alloys is interpreted in Fig.(8). However, in the

Ag, and Cu free alloy, the values of ϵ_T are lower with increasing temperature at all strain rates. This disagreement in the correlation between stress-strain and temperature appears to depend on the alteration in the microstructure of the samples. It is clear that Sn-9Zn-1.5Ag is more elongation than Sn-9Zn-1.5Ag-0.7Cu.

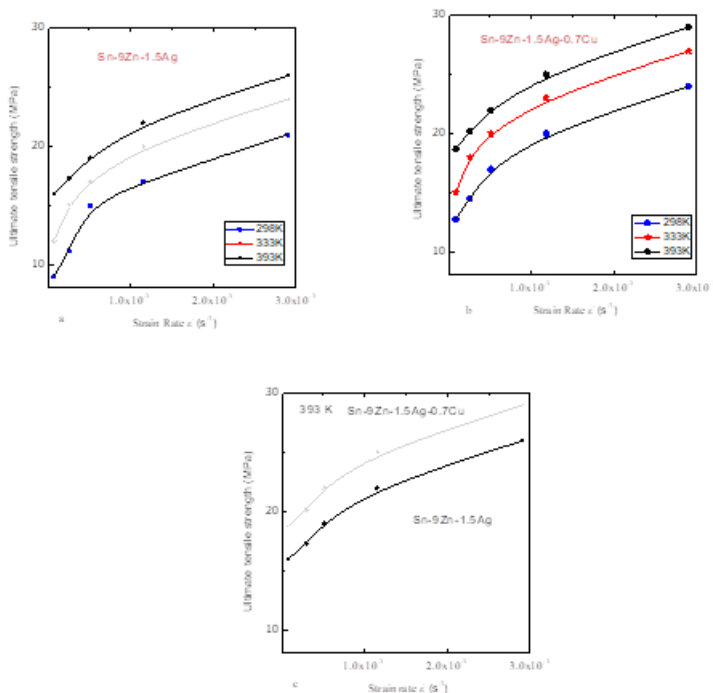


Fig.(5) a, b : The variation of the ultimate tensile stress (UTS) with strain rate at different working temperature for tested solder alloys; c) The variation of (UTS) at fixed temperature 393 K.

We can sight that; strain rate is inversely proportional with fracture strain (ϵ_f) as ordinance in Fig. (9). It was celebrated that the activation energy may be estimated from the connection between \ln (fracture strain ϵ_f) with $1000/T$ at several working temperature are illustrated in Fig.(10 a, b). The value of activation energy with temperature for solders is described in Fig.(10c). The activation energy of Sn-9Zn-1.5Ag-0.7Cu alloy is higher than that of Sn-9Zn-1.5Ag; there fort first samples is more strengthening (less in elongation) than the second.

3.2-Stress exponent

The activation energy and stress exponent (n) are significant thermodynamic and mechanical factors to characterize the creep deformation mechanisms of samples [27]. In general, the deformation afthought by diffusion mechanism can be determines by [21]:

$$\dot{\epsilon} = A \sigma^n \tag{2}$$

where $\dot{\epsilon}$ is the strain rate, σ is the stress and A is the material-dependent constant [27]. The deformation mechanism is diffusion it can be characterised by equation (2) [23].

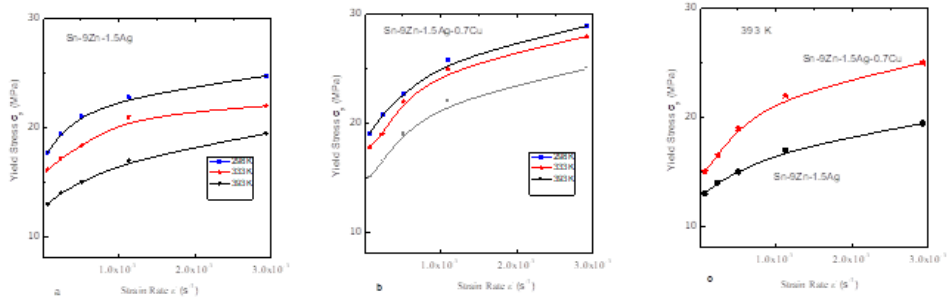


Fig.(6) a, b : The variation yield strength (σ_y) with strain rate at different working temperature for tested solder alloys; c) The variation of (σ_y) at fixed temperature 393 K.

Figure (11) shows a linear relationship between UTS and strain rate (log–log plot), and the slope of each line (fitted to the experimental data) gives the so-called stress exponent, n. The n values at different temperatures for the tested alloys are listed in Table 2,3. It is clear that the value of stress exponent, n of Sn-9Zn-1.5Ag-0.7Cu alloy is above than that of Sn-9Zn-1.5Ag. In this paper (stress exponent $n \geq 4$), therefore the controlling mechanism is dislocation climb [28]. Fig.(12) a. demonstrated XRD manner for first alloy where Ag, Zn, and Sn appear and (b) for Sn-9Zn-1.5Ag-0.7Cu; the Ag_3Sn morphology was confirmed in the XRD model of tested samples, showing the effective alloying of Sn and Ag after the melting process. At the same time, the Cu_6Sn_5 and Cu_3Sn phases were formed, which were due to the alloying of Sn and Cu in the Sn-9Zn-1.5Ag-0.7Cu alloy. Furthermore, the comparative density of β -Sn was established to be slightly lowered with the increase of Cu, due to the structure of Cu_6Sn_5 and Cu_3Sn phases.

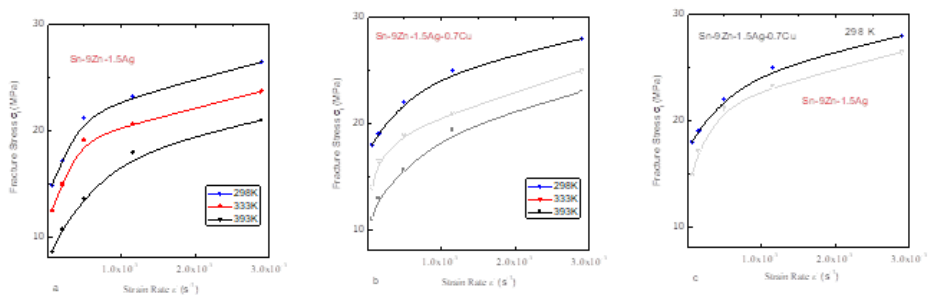


Fig.(7) a, b : The variation of fracture strength (σ_f) with strain rate at different working temperature for tested solder alloys; c) The variation of (σ_f) at fixed temperature 298 K.

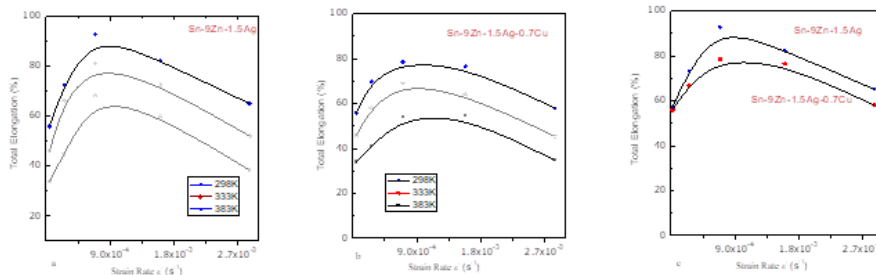


Fig.(8) a, b : The variation of total elongation (ϵ) with strain rate at different working temperature for tested solder alloys; c) The variation of total elongation (ϵ) at fixed temperature 298 K.

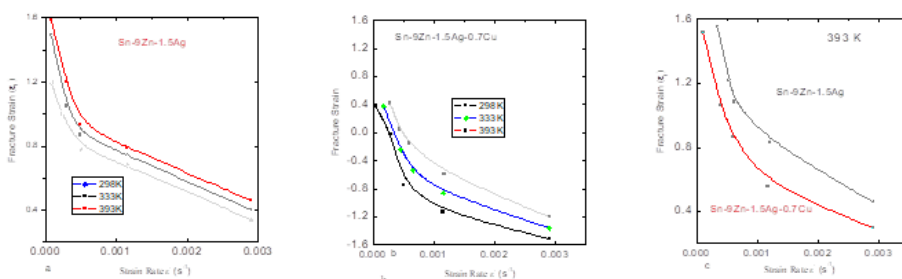


Fig.(9) a, b : The variation fracture strain (ϵ_f) with strain rate at different working temperature for tested solder alloys; c) The variation of fracture strain (ϵ_f) at fixed temperature 393 K.

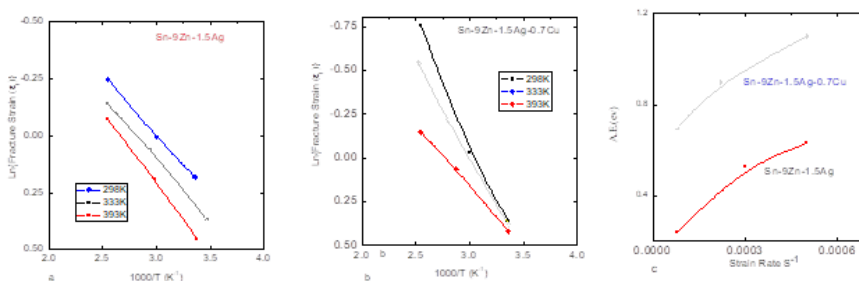


Fig.(10): a, b: the relation between \ln fracture strain (ϵ_f) with $1000/T$ at different working temperature for tested alloys,c; The activation energy with strain rate for tested alloys.

Fig.(13) a: represented EDS images of the tested alloys, the microstructure composed of β -Sn areas, fine Ag_3Sn precipitates. In Fig.3.b, analysis of the tested alloys. This observation implies that the needle-like phases are the Cu_6Sn_5 IMCs, while the Cu_3Sn IMC, and also, the fine particles dispersed in the β -Sn phase were determined. In Fig.(14) SEM images of the alloys microstructure composed of light gray areas of Cu_6Sn_5 IMCs and dark network-like eutectic regions of β -Sn and

white area of Ag_3Sn . A small addition of Ag into the Sn–9Zn alloy produced many small spheroidal particles within the like-eutectic regions and they were determined to be Ag_3Sn IMC phase. The reason may be that the Cu addition promotes a high nucleation density of the second phase in the Sn–9Zn during solidification.

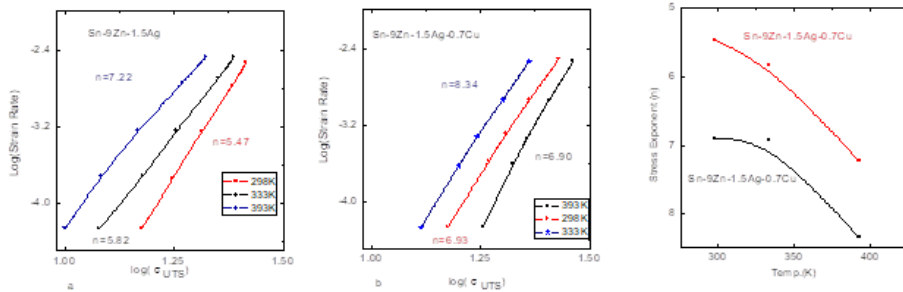


Fig.(11): a,b: shows a line are relationship between UTS and strain rate (log–log plot),and the slope of each line (fitted to the experimental data); c gives the so-called stress exponent.

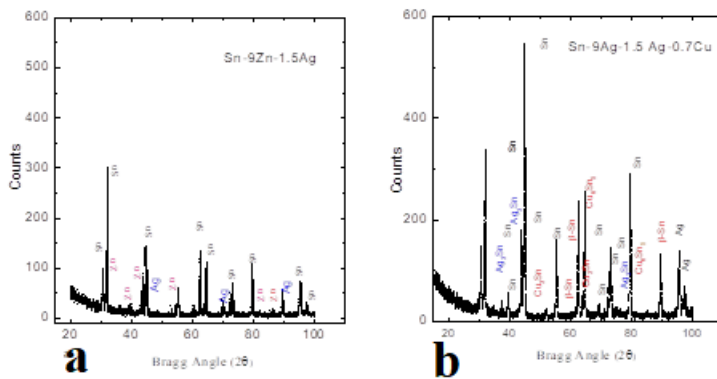


Fig. (12) a. XRD pattern for Sn-9Zn-1.5Ag alloy where Ag, Zn, and Sn appear and (b) for Sn-9Zn-1.5Ag-0.7Cu mainly composed of β -Sn phase exhibited additional IMCs such as Ag_3Sn , Cu_6Sn_5 .

Table (2): Tensile parameters of Sn-9Zn-1.5Ag

Temp. K	Y	σ_y	σ_f	UTS	ϵ_f	n	$\epsilon_t\%$
298	2894	24.75	26.74	46	1.59	5.47	93
333	2312	22	23.7	24	1.49	5.82	81
393	1647	19.45	21	21	1.2	7.22	68

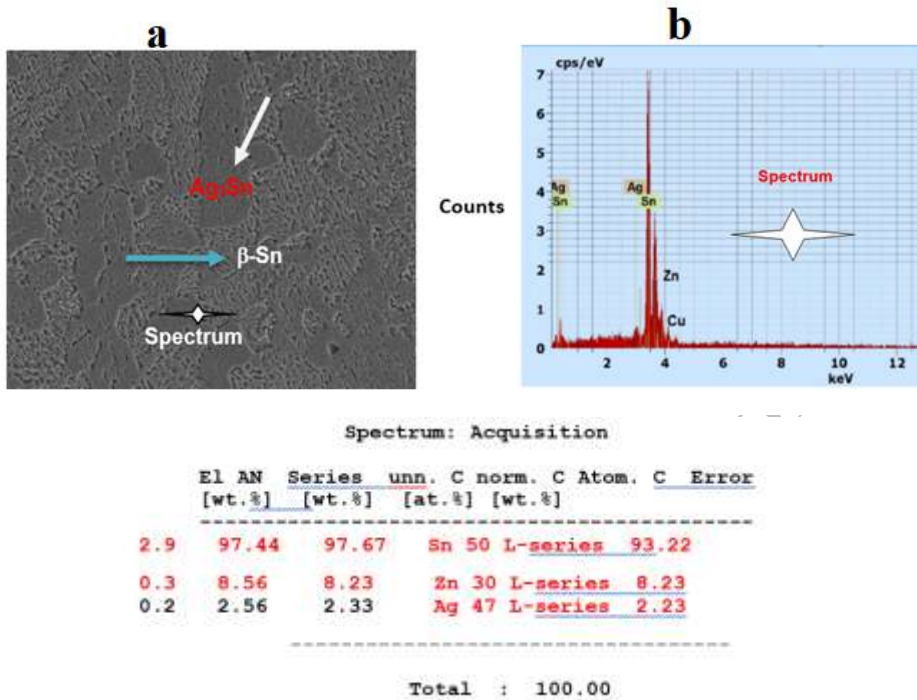


Fig.(13) a: represented SEM images of the tested alloys, the microstructure composed of β -Sn areas, fine Ag_3Sn precipitates. In Fig.3.b, EDS analysis of the tested alloys.

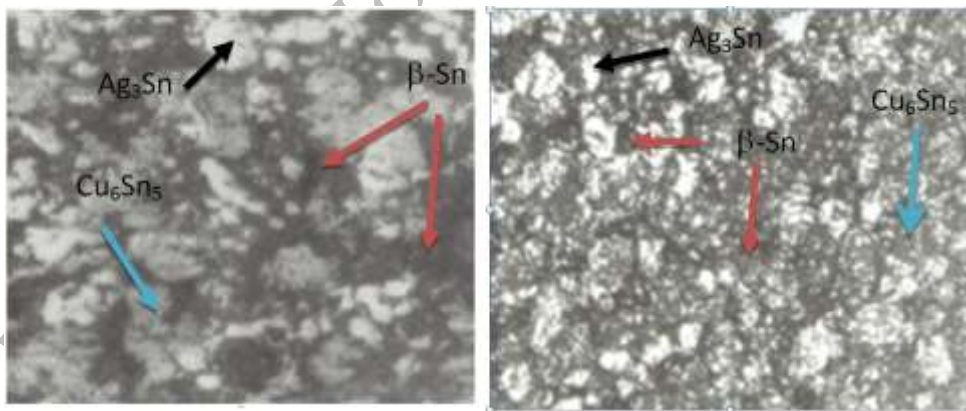


Fig.(14):The SEM images of the alloys microstructure composed of light gray areas of Cu_6Sn_5 IMCs and dark network-like eutectic regions of β -Sn and white area of Ag_3Sn .

Table (3): Tensile parameters Sn-9Zn-1.5Ag-0.7Cu

Temp. K	Y	σ_y	σ	UTS	ϵ_f	n	$\epsilon_t\%$
298	1511	29	2	29	1.5	6.9	78.
333	1300	28	2	27	1.4	6.9	69
393	972	25	2	24	1.4	8.3	53

Conclusion

- 1- The total elongation ϵ_T are decrease with rising temperature at all strain rates.
- 2- This disagreement in the correlation between stress-strain and temperature appears to depend on the alteration in the microstructure of the samples.
- 3- The Sn-9Zn-1.5Ag-0.7Cu is more strengthening than Sn-9Zn-1.5Ag; i.e. it is clear that Sn-9Zn-1.5Ag is more elongation than Sn-9Zn-1.5Ag-0.7Cu; therefore the activation energy of Sn-9Zn-1.5Ag is minimize than second alloy.

References:

1. M. Abteu, G. Selvaduray, *Mater. Sci. Eng.*, R **27**, 95 (2000).
2. V. Chidambaram, J. Hattle, J. Hald, *Microelectron. Eng.*, **88**, 981 (2011).
3. A.N. Fouda, E.A. Eid; *Materials Science & Engineering, A* **632**, 82 (2015). 7
4. H. Mavoori, S. Jin, *J. Electron. Mater.*, **27** (11), 1216 (1998).
5. L.C. Tsao, S.Y. Chang, *Mater. Des.* **31**, 990 (2010).
6. H. Mavoori, *JOM* **52** (6), 29 (2000).
7. J. Shen, Y.C. Chan, *Microelectron. Reliab.* **49**, 223 (2009).
8. J. Rodney, McCabe, E. Morris, *Metall. Mater. Trans. A* **33A**, 1531. (2002).
9. M.D. Mathew, H. Yang, S. Movva, K.L. Morty, *Metall. Mater. Trans. A* **36A**, 99. (2005).
10. A. Verma, SP. Tewari, J. Prakash, *Journal of Engineering Science and Technology.*, **3**(6):5215 (2011).
11. M. Y. Salem and A.S.Mahmoud, Egypt. J. Solids, Vol. (40), 39, (2017)
Verissimo NC, Brito C, Santos WLR, Cheung N, Spinelli JE, Garcia A., *Journal of Alloys and Compounds.* **662**, 1 (2016).
12. Zhang B, Li X, Wang T, Liu Z., *Materials Science and Engineering: A.* **674**, 242 (2016).
13. Liu K, Jiang Z, Zhao J, Zou J, Chen Z, Lu D. *Journal of Alloys and Compounds.*; **612**, 221 (2014).

14. A.A. El-Daly, A. Fawzy, S.F. Mansour, M.J. Younis, *Mater Sci Eng A*; **578**, 62, (2013).
15. A.A. El-Daly, A. Fawzy, S.F. Mansour, M.J. Younis, *J. Mater Sci: Mater Electron* **24**; 2976 (2013).
16. M.Y. Salem, *Egypt. J. Solids*, Vol. (**39**); 107 (2016).
17. Salem M.Y. *International Journal of New Horizons in Physics* Vol. **4**, No. 2, 21 (2017).
18. C. Andersson, P. Sun, J. Liu, *J. Alloys Compd.*, **457**, 97 (2008).
19. F. Zhu, H. Zhang, R. Guan, S. Liu, *Microelectron. Eng.*, **84**, 144 (2007).
20. Q.S. Zhu, Z.G. Wang, S.D. Wu, J.K. Shang, *Mater. Sci. Eng. A* **502**, 153 (2009).
21. A.A. El-Daly, *Phys. Stat. Sol., A* **201** (9), 2035 (2004).
22. G.H. Edward, M.F. Ashby, *Acta Metall.*, **27**, 1505 (1979).
23. A.A. El-Daly, A.E. Hammad, *Mater. Sci. Eng., A* **527**, 5212 (2010).
24. A.A. El-Daly, A.E. Hammad, *Journal of Alloys and Compounds*, **509**, 8554 (2011).
25. Fawzy. A; Effect of Zn addition, strain rate and deformation temperature on the tensile properties of Sn-3.3 wt.% Ag solder alloy *Materials Characterization* **58**, 323 (2007).
26. Z. Liang, X. Song-bai, G. Li-li, Z. Guang, C. Yan, Y. Sheng-lin, S. Zhong, *Trans. Nonferr. Met. Soc. Chin.* **20**, 412 (2010).
27. R. Mahmudi, A.R. Geranmayeh, H. Khanbareh, N. Jahangiri, *Mater. Des.* **30**, 574 (2009).